

# Electrophoretic deposition of surface-modified titanate nanosheets via layer-by-layer assembly and deposited film properties

Atsunori Matsuda<sup>a,\*</sup>, Tomohisa Kambayashi<sup>a</sup>, Yusuke Daiko<sup>b</sup>,  
Hiroyuki Muto<sup>a</sup>, Mototsugu Sakai<sup>a</sup>

<sup>a</sup> Department of Materials Science, Toyohashi University of Technology, 1-1 Hibarigaoka, Tempaku, Toyohashi, Aichi 441-8580, Japan

<sup>b</sup> Department of Materials Science and Chemistry, University of Hyogo, 2167 Syosya, Himeji, Hyogo 671-2201, Japan

Available online 8 October 2009

## Abstract

The surface of  $\text{H}_2\text{Ti}_4\text{O}_9 \cdot x\text{H}_2\text{O}$  titanate nanosheets was modified using the sulfonated tetrafluoroethylene-based polymer Nafion<sup>®</sup>, via layer-by-layer assembly. The surface modification allowed the titanate nanosheets to be highly dispersed in hydrophobic organic solvents. Thick films of surface-modified nanosheets were prepared on indium tin oxide (ITO)-coated glass substrates as a negative electrode by electrophoretic deposition. The thickness of the films increased with increasing deposition time and grew to more than 8  $\mu\text{m}$  in 600 s under potentiostatic conditions at 7.5 V. The electrophoretically deposited thick films showed significant hydrophobicity with contact angle for water 95°, and enhanced adsorption and higher photocatalytic activity for hydrophobic dyes such as thionine than those of thick films prepared from unmodified titanate nanosheets.  
© 2009 Elsevier Ltd. All rights reserved.

**Keywords:** Titanate nanosheet; Electrophoretic deposition; Layer-by-layer assembly; Hydrophobicity; Photocatalytic activity

## 1. Introduction

Two-dimensional titanate nanosheets have been synthesized by ion-exchange and delamination of layered alkali titanate crystallites into a single layer.<sup>1</sup> Titanate nanosheets show high photocatalytic activity, distinctive solid acidity, good ion-exchange properties, and large intercalation capacity, owing to their high specific surface area, high activity and ultra-thin dimensions. Syntheses, structures and characteristics of several types of nanosheets from titanates such as  $\text{H}_2\text{Ti}_3\text{O}_7$ ,  $\text{H}_2\text{Ti}_4\text{O}_9$ , and  $\text{H}_2\text{Ti}_5\text{O}_{11}$  have been reported.<sup>2–4</sup> Thin flakes and porous aggregates of titanate are obtainable from the colloidal nanosheet suspension by centrifugation and drying, whereas immobilization of the titanate nanosheets on substrates, *i.e.*, the formation of thin or thick films of titanate nanosheets on substrates is essential for practical applications. Formation of titania nanosheet/polycation composite films based on electrostatic interaction by layer-by-layer (LbL) assembly has been reported.<sup>5</sup> In addition, it has been reported that titania nanosheet-precipitated films can be formed by dissolution and re-precipitation of sol–gel derived silica-titania gel films by hot

water treatment in external fields such as vibration and an electric field.<sup>6</sup>

Electrophoretic deposition (EPD) is a promising technique for preparing films more than 1  $\mu\text{m}$  in thickness, and has been widely used for the fabrication of functional coatings for practical applications including the use of nanoparticles, nanotubes and nanorods.<sup>7</sup> We have reported the preparation of layered titanate thick films from tetratitanate ( $\text{H}_2\text{Ti}_4\text{O}_9$ ) nanosheet colloidal suspension by EPD.<sup>8</sup>  $\text{H}_2\text{Ti}_4\text{O}_9$  nanosheet is composed of corrugated ribbons of edge-sharing  $\text{TiO}_6$  octahedral units, which join corners to form stepped sheets separated by  $\text{H}^+$  ions in an inter-sheet. By maintaining neutral pH of the aqueous suspension, uniformly dense layered titanate thick films were deposited on a conductive substrate as a positive electrode owing to suppression of the electrolysis of water. The resultant layered films showed strong adsorption for hydrophilic organic dye, and high photocatalytic activity under ultraviolet (UV) irradiation.

In the present study, we have prepared hydrophobic and photocatalytic layered titanate thick films on indium tin oxide (ITO)-coated glass substrates by EPD, from surface-modified tetratitanate nanosheets in organic solvent suspensions. Surface modification of titanate nanosheets was performed with a sulfonated tetrafluoroethylene-based polymer, Nafion<sup>®</sup>, via LbL assembly to provide hydrophobic titanate nanosheets, and to permit facile dispersion of titanate nanosheets in organic solvents

\* Corresponding author. Tel.: +81 532 44 6799.

E-mail address: [matsuda@tutms.tut.ac.jp](mailto:matsuda@tutms.tut.ac.jp) (A. Matsuda).

without aggregation. LbL assembly was conducted through an electrostatic interaction: oppositely charged materials such as polyelectrolytes were alternately deposited on a charged substance, and an insoluble polymer complex a few nanometers in thickness was formed at room temperature and ambient atmosphere.<sup>9,10</sup> Changes in the  $\zeta$ -potential of the negatively charged titanate nanosheet surface, formed by LbL assembly, were observed. The hydrophobicity of the electrophoretically deposited thick films was evaluated from the contact angle for water, and adsorption of hydrophilic and hydrophobic dyes. The photocatalytic activity of the deposited thick films was examined by decomposition and/or bleaching of the adsorbed dyes during UV irradiation.

## 2. Experimental

### 2.1. Preparation of titanate nanosheets and deposition of ultrathin Nafion layer

A colloidal suspension of tetratitanate ( $\text{H}_2\text{Ti}_4\text{O}_9$ ) nanosheets (2.6 wt%) was prepared from layered titanates by exfoliation using *N,N*-dimethylethanolamine (DMEA).<sup>8</sup> The titanate nanosheet sol was neutralized with boric acid then washed with deionized water. Neutralization with the weak acid was found to be effective to control the pH of the suspension and suppress dissolution of titanate nanosheets. The thickness of the titanate nanosheets was measured using an atomic force microscope (AFM, NPX 200, SII NanoTechnology Inc., Japan).

For the surface modification of negatively charged titanate nanosheets with negatively charged Nafion, the use of a positively charged polymer electrolyte is very important. In this study, poly(diallyldimethylammonium chloride) (PDDA, weight average molecular mass  $M = (1-2) \times 10^5 \text{ g mol}^{-1}$ , Sigma-Aldrich Co., Ltd., USA) was used as a cationic polymer electrolyte for LbL assembly. A Nafion<sup>®</sup> solution (10 wt%, Wako Pure Chemical Industries, Ltd., Japan) was used as purchased. PDDA aqueous solution ( $10 \text{ mg mL}^{-1}$ ) containing 0.5 M NaCl and Nafion solution in methanol ( $2 \text{ mg mL}^{-1}$ ) were used for the LbL deposition.

PDDA solution (20 mL) was added to the diluted titanate nanosheet colloidal suspension (1.3 wt%, 20 mL) and the mixture stirred at 600 rpm for 30 min at room temperature using a magnetic stirrer, to obtain a homogeneous suspension. The PDDA-modified titanate nanosheet suspension was centrifuged at 1000 rpm for 5 min (#5922, Kubora Co., Ltd., Japan). The methanolic Nafion solution (20 mL) was added to the centrifuged ( $\sim 8.4 \times g$ ) PDDA-modified titanate nanosheet suspension, then the mixture was again stirred at 600 rpm for 30 min at room temperature. The Nafion/PDDA-modified titanate nanosheet suspension was then centrifuged under the same conditions as those for PDDA-modification. The LbL assembly process, as described above, for titanate nanosheets with PDDA and Nafion was repeated three times. After each deposition step, the centrifuged nanosheets were washed three times with deionized water to remove excess PDDA and Nafion. Finally, (Nafion/PDDA)<sub>3</sub>-modified titanate nanosheets were dried at room temperature in an ambient atmosphere.

The surface-modified titanate nanosheets thus obtained were experimentally found to show high dispersibility in organic solvents such as methanol, ethanol, *N*-methylpyrrolidone and 2-methoxyethanol, without aggregation or agglomeration.

A quartz crystal microbalance (QCM, UEQ-400Easy, USI Co., Ltd., Japan) was used for monitoring the adsorption of PDDA and Nafion layers. A gold-coated QCM electrode (AT-cut) with resonance frequency 9 MHz was used. Before each QCM experiment, the QCM electrode was cleaned with piranha solution (98%  $\text{H}_2\text{SO}_4$ :30%  $\text{H}_2\text{O}_2 = 3:1$ , v/v), rinsed with pure water, and dried with nitrogen gas. The alternate deposition of PDDA and Nafion multilayers on the titanate nanosheets, which were deposited on the QCM electrode with PDDA, was monitored by QCM. Changes in the surface charge of the titanate nanosheet with LbL deposition of PDDA and Nafion were measured using a  $\zeta$ -potential analyzer (ELS-Z1NS, Otsuka Electronics Co., Ltd., Japan). An average of five measurements at the stationary level was taken for each data point.  $\zeta$ -potential measurement was conducted in deionized water.

### 2.2. Electrophoretic deposition

An ethanol suspension of (Nafion/PDDA)<sub>3</sub>-modified titanate ( $\text{H}_2\text{Ti}_4\text{O}_9$ ) nanosheets (3.5 wt%) was employed for EPD, and an aqueous suspension of unmodified titanate nanosheets (2.6 wt%) neutralized with boric acid prior to LbL was used for EPD for comparison.

A pair of indium tin oxide (ITO)-coated glass substrates, with area  $10 \text{ mm} \times 20 \text{ mm}$ , was placed in the suspension so that the distance between the substrates was 15 mm. The applied voltage was maintained by a potentiostat/galvanostat (SI1287, Toyo Co., Ltd., Japan) at potentiostatically 7.5 V DC and the deposition time of electrophoresis was adjusted in the range 50–600 s. The films deposited on the substrates were pulled up at a speed of  $1 \text{ mm s}^{-1}$  and dried at room temperature overnight. In addition, the voltage was scanned at  $200 \text{ mV s}^{-1}$  to measure the electric current during electrophoretic deposition, which was analyzed in relation to the results of current–voltage curves to examine the over-potential of the gas generation during EPD. The microstructure of electrodeposited films was observed using a scanning electron microscope (S-4800, Hitachi High-Tech., Co., Ltd., Japan), an X-ray diffractometer (RINT 2000, Rigaku Co., Ltd., Japan) and an IR spectrometer (FT/IR-7300, WS/IR-7300, Jasco, Co., Ltd., Japan).

### 2.3. Evaluation of film properties

Changes in water contact angle for the electrophoretically deposited films were measured using a contact angle measuring instrument (CA-C, Kyowa Surface Science Co., Ltd., Japan).

Aqueous solutions of methylene blue (MB) and thionine (TN) were used as indicators to evaluate the photocatalytic activity of the titanate nanosheet EPD films: MB and TN were selected as hydrophilic and hydrophobic substances, respectively. The concentration of the MB and TN solutions was  $10^{-5} \text{ M}$ . MB or TN aqueous solution (10 mL) was poured into a petri dish, and the titanate nanosheet films deposited on ITO-coated glass

substrates were soaked in the MB or TN solution for 30 min in the dark. After the substrates with films were removed from dye solution and dried with flowing nitrogen gas, the capacity of the films to adsorb MB or TN was measured by UV–Vis spectrophotometry (V-560, Jasco Co., Ltd., Japan). The films were soaked in the MB or TN solution again and the changes in absorbance of the solutions with UV irradiation were repeatedly measured every 30 min for 3 h. Subsequently, the films with adsorbed MB or TN were irradiated with UV light in the ambient atmosphere using a black light (with intensity of illumination  $1.0 \text{ mW cm}^{-2}$ ) for a given irradiation time, and the changes in the absorbance of the films were measured using a UV–vis spectrophotometer over a 24 h period.

### 3. Results and discussion

#### 3.1. LbL modification of titanate nanosheets

The titanate in the prepared nanosheets was identified as tetratitanate ( $\text{H}_2\text{Ti}_4\text{O}_9 \cdot n\text{H}_2\text{O}$ ) from XRD measurements. The thickness and size of the titanate nanosheets were estimated as about 0.9 nm and  $10 \mu\text{m}$ , respectively, from AFM observation (Fig. 1). Ultrathin layers of positively charged PDDA and negatively charged Nafion were alternately deposited on the titanate nanosheets via LBL assembly. Fig. 2 shows the incremental film growth of PDDA and Nafion multilayers on titanate nanosheets as monitored using a QCM. In the first step, positively charged PDDA was deposited on the gold-coated QCM electrode since the QCM electrode was negatively charged in aqueous solution. In the second step, negatively charged titanate nanosheet was deposited on the PDDA-coated QCM electrode and then positively charged PDDA and negatively charged Nafion were alternately deposited on the QCM electrode. The amounts of deposited PDDA and Nafion increased linearly with the num-

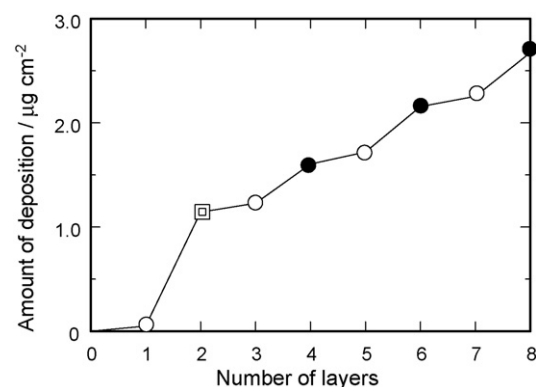


Fig. 2. Changes in the amounts of PDDA, titanate nanosheet, and Nafion deposited on an Au-coated QCM electrode by LbL assembly. Open circles, square, and closed circles represent PDDA, titanate nanosheet, and Nafion, respectively.

ber of layers, indicating that multiple PDDA/Nafion bilayers were deposited regularly. The amounts of deposited PDDA and titanate nanosheet on the QCM electrode in the first and second steps were calculated as  $0.049$  and  $1.144 \mu\text{g cm}^{-2}$ , respectively. From the deposition weight and the roughly estimated density of about  $4 \text{ g cm}^{-3}$  for titanate, the thickness can be calculated as  $2.9 \text{ nm}$ , which corresponds to several sheets of titanate nanosheet. In addition, the average amounts of PDDA and Nafion deposited on the titanate nanosheets on the QCM electrode in each operation from the 3rd to the 8th steps were calculated as  $0.099$  and  $0.411 \text{ mg cm}^{-2}$ , respectively.

The  $\zeta$ -potential of titanate nanosheet was  $-23 \text{ mV}$  in a neutral aqueous solution before LbL modification, increased to  $+52 \text{ mV}$  after the first deposition of PDDA and decreased to  $+3 \text{ mV}$  after deposition of Nafion. After deposition of PDDA in the second step, the  $\zeta$ -potential tended to level off at about  $+50 \text{ mV}$  during the repeated deposition of PDDA and Nafion, which is probably due to the strong cationic nature of PDDA. These results agreed

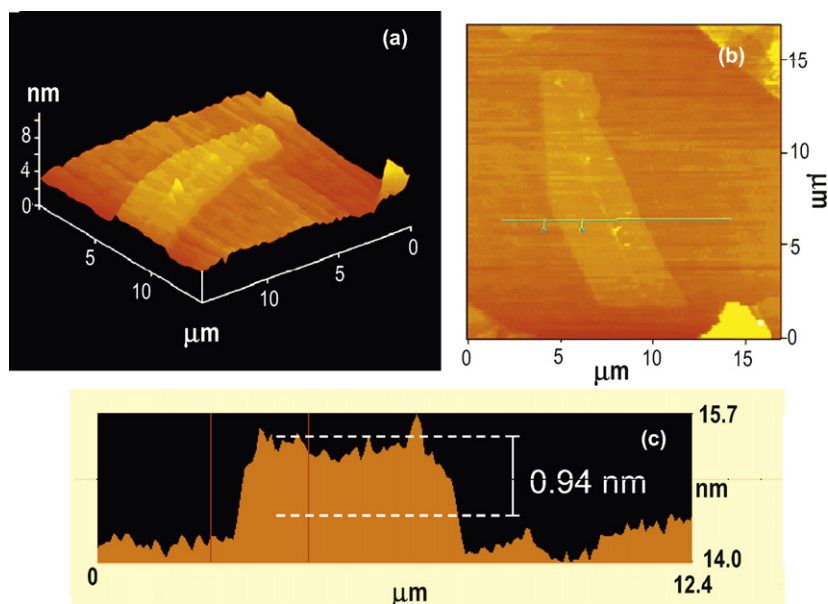


Fig. 1. AFM images of the titanate nanosheet, and the evaluation of thickness and size of the titanate nanosheet: (a) 3D-image, (b) plan view, and (c) cross-sectional view.

with the experimental results that the Nafion-modified titanate nanosheets were deposited not on the positive electrode but on the negative electrode substrate during EPD processing.

### 3.2. EPD of LbL-modified titanate nanosheets

The potentiodynamic current–voltage curves at  $200 \text{ mV s}^{-1}$  for EPD of the films from the aqueous suspension of unmodified titanate nanosheets and the ethanol suspension of LbL-modified titanate nanosheets, are shown in Fig. 3(a). Titanate nanosheet deposition was observed at the positive electrode for the unmodified, negatively charged titanate nanosheets and at the negative electrode for the LbL-modified, positively charged titanate nanosheets. At a given applied voltage, the current density of EPD using the LbL-modified titanate nanosheet suspension was lower by about 3 orders of magnitude than that of EPD using the unmodified titanate nanosheet suspension. The lower current density of the LbL-modified titanate nanosheet suspension can be ascribed to the higher resistivity and lower dielectric constant of the ethanol suspension. For both cases, the electric currents increased with increase in the applied voltage. Changes in the current densities under potentiostatic conditions at 7.5 V for EPD using an aqueous suspension of the unmodified titanate nanosheets, and an ethanol suspension of the LbL-modified titanate nanosheets, are also shown in Fig. 3(b). A drastic decrease in the current density was observed at around 100 s for the unmodified titanate nanosheets, which suggests a

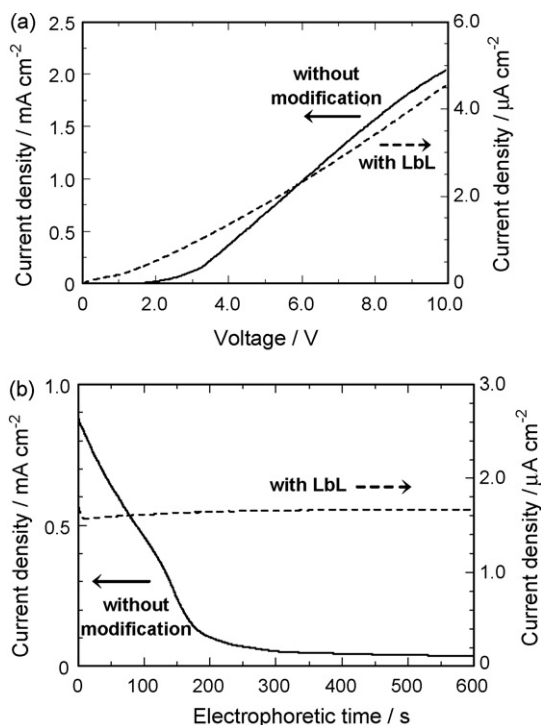


Fig. 3. (a) Potentiodynamic current–voltage curves at  $200 \text{ mV s}^{-1}$  for EPD films which were prepared by using an unmodified titanate nanosheet aqueous suspension (solid line) and an LbL-modified titanate nanosheet ethanol suspension (broken line); (b) changes in the current densities under a potentiostatic condition at 7.5 V for EPD using the unmodified titanate nanosheet aqueous suspension (solid line) and an LbL-modified titanate nanosheet ethanol suspension (broken line).

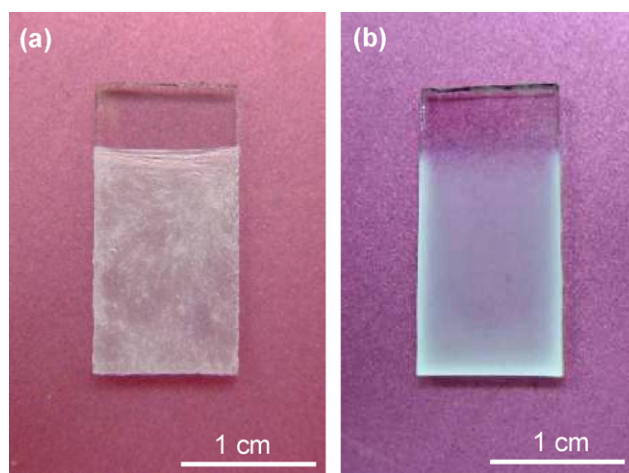


Fig. 4. Optical microphotographs of (a) unmodified titanate and (b) LbL-modified titanate films formed on ITO-coated glass substrates by EPD at potentiostatically 7.5 V for 100 s.

large increase in resistivity of the unmodified titanate nanosheet films deposited on the ITO/glass substrate. On the other hand, the current density was almost constant during deposition of the LbL-modified titanate nanosheets, which can be ascribed to the open structure of the deposited film and the slow deposition rate of those nanosheets. The thickness of the deposited films after 600 s was  $22 \mu\text{m}$  for the unmodified titanate nanosheets and  $8.5 \mu\text{m}$  for LbL-modified titanate nanosheets. When the applied voltage was 2 V in the potentiostatic EPD, almost no deposition was observed for the unmodified titanate nanosheets, whereas continuous deposition was observed for the LbL-modified titanate nanosheets, and the thickness reached  $8 \mu\text{m}$  after 600 s.

Fig. 4 shows optical microscope images of (a) unmodified titanate, and (b) LbL-modified titanate, formed on ITO-coated glass substrates by EPD. The applied voltage and deposition time were 7.5 V and 100 s, respectively. While both films were translucent, the surface of the LbL-modified film seemed more homogeneous than that of the unmodified film.

Fig. 5 shows FE-SEM images of the surface and cross-section of the titanate nanosheet films prepared from (a) unmodified titanate, and (b) LbL-modified titanate, by EPD. The EPD conditions were the same as for Fig. 3. Shriveled textures with domains were observed for the surface of the unmodified titanate film (Fig. 5(a<sub>1</sub>)), and fine crinkled textures without domains occurred for the LbL-modified titanate film (Fig. 5(b<sub>1</sub>)). The unmodified titanate nanosheets were stacked to form a dense film about  $3 \mu\text{m}$  in thickness (Fig. 5(a<sub>2</sub>)), whereas the LbL-modified titanate nanosheets were undulated to form a film about  $2 \mu\text{m}$  thick (Fig. 5(b<sub>2</sub>)). For both films, defects such as domes, hollows and peelings caused by generation of  $\text{O}_2$  or  $\text{H}_2$  gas at the surface of the electrodes were not observed.

The changes in thickness with deposition time at 7.5 V of the EPD films prepared from the unmodified titanate nanosheet aqueous suspension, and from the LbL-modified titanate nanosheet ethanol suspension, are shown in Fig. 6. The thickness of each film was evaluated using cross-sectional SEM at the center of the ITO-coated glass substrate ( $10 \text{ mm} \times 20 \text{ mm}$ ).



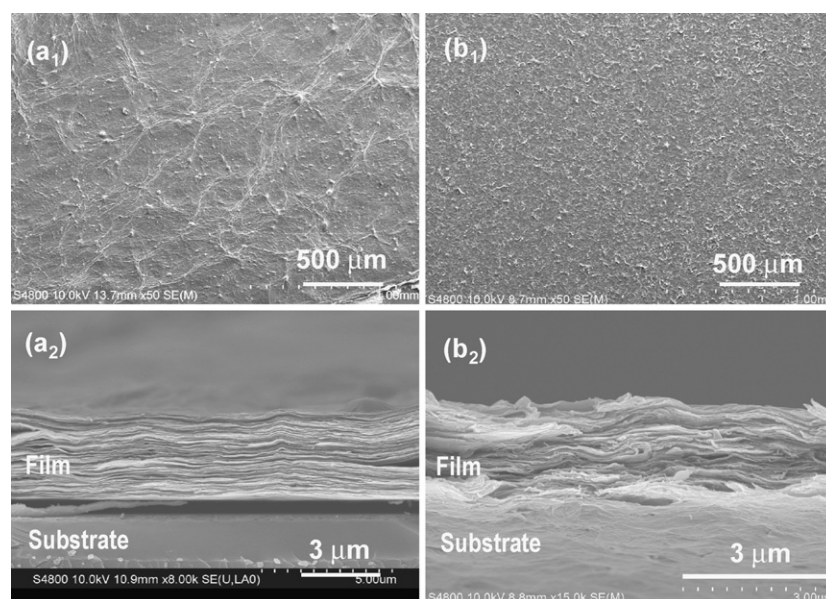


Fig. 5. FE-SEM images of the titanate nanosheet films formed on ITO-coated glass substrates by EPD at potentiostatically 7.5 V for 100 s. (a<sub>1</sub>) Surface and (a<sub>2</sub>) cross-section of the film prepared from unmodified titanate, and (b<sub>1</sub>) surface and (b<sub>2</sub>) cross-section of the film prepared from LbL-modified titanate.

Linear relationships between film thickness and deposition time were observed for both suspensions. After deposition for 600 s the film thickness reached 22  $\mu\text{m}$  for unmodified titanate nanosheets, and 8.5  $\mu\text{m}$  for LbL-modified titanate nanosheets after the same deposition time. According to the Helmholtz–Smoluchowski equation, the steady rate of particles in colloidal suspension is proportional to both the dielectric constant and zeta-potential. Therefore, the smaller dielectric constant of ethanol and smaller value of the  $\zeta$ -potential of LbL-modified titanate nanosheet have caused the lower deposition rate of the modified titanate nanosheets.

### 3.3. Properties of EPD films of LbL-modified titanate nanosheets

Since titania ( $\text{TiO}_2$ ) is hydrophilic and shows photocatalytic activity, titania-based materials have been extensively stud-

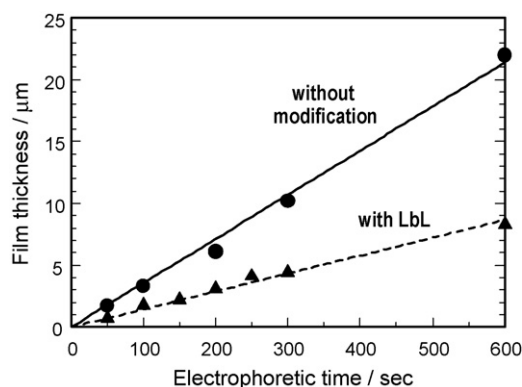


Fig. 6. Relationship between film thickness and deposition time at potentiostatically 7.5 V. Closed circles and triangles are for unmodified titanate nanosheet aqueous suspension and the LbL-modified titanate nanosheet ethanol suspension, respectively.

ied for applications including self-cleaning, anti-fogging and environmental purification.<sup>11,12</sup> Surface modification of titanate nanosheets provides not only a high degree of dispersion in organic solvents but also hydrophobicity of the resultant EPD films. The combination of hydrophobic character and photocatalytic activity is expected to lead to new applications of the multifunctional surfaces.<sup>13</sup>

Contact angles for water of the EPD films prepared from the unmodified and LbL-modified titanate nanosheets are compared in Fig. 7. Both films were prepared under applied voltage at 7.5 V and deposition time for 100 s. The EPD film prepared from LbL-modified titanate nanosheets shows appreciable hydrophobicity with contact angle for water of about  $95^\circ$ , which is much higher than that ( $26^\circ$ ) of the film prepared from unmodified nanosheets. Such significant hydrophobicity with high contact angle for water can be ascribed to the very low surface energy of the fluoroalkyl chain in Nafion. However, titania photocatalytically decomposes coexistent organic moieties, which often causes degradation of the hydrophobicity of titania-based materials. Consequently, an important concern is the durability of hydrophobic EPD film obtained from LbL-modified titanate nanosheets. The changes in contact angle for water of the EPD films prepared from unmodified titanate nanosheets and the LbL-modified titanate nanosheets are shown in Fig. 8: the intensity of illumination was  $1.0 \text{ mW cm}^{-2}$ . For both films, the contact angles for water decreased with increase in UV irradiation time, indicating that titanate nanosheet has photocatalytic activity to decompose the organic moieties at the surface of the films. The EPD film obtained from unmodified titanate nanosheets showed superhydrophilicity with a contact angle for water of about  $4^\circ$  after UV irradiation for 60 min. By contrast, the contact angle for water of the EPD film obtained from LbL-modified titanate nanosheets decreased from  $95^\circ$  to  $85^\circ$ , and the hydrophobic EPD film retained a relatively high contact angle for water of about  $67^\circ$  even after 48 h (2880 min) irradiation.

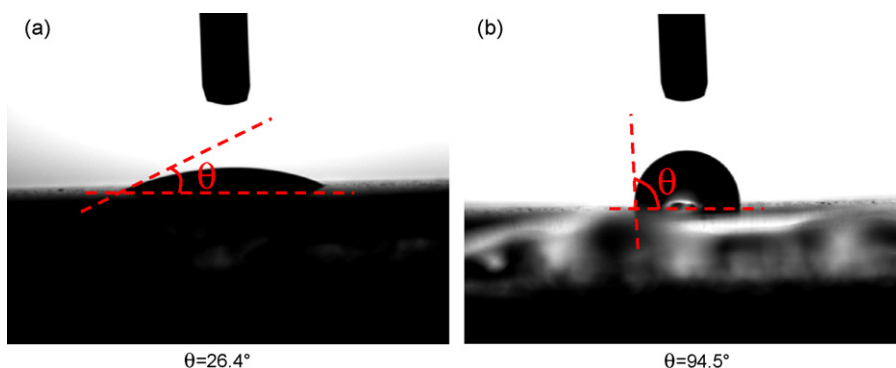


Fig. 7. Optical microscope images of water droplets on the EPD films prepared from the (a) unmodified and (b) LbL-modified titanate nanosheets.

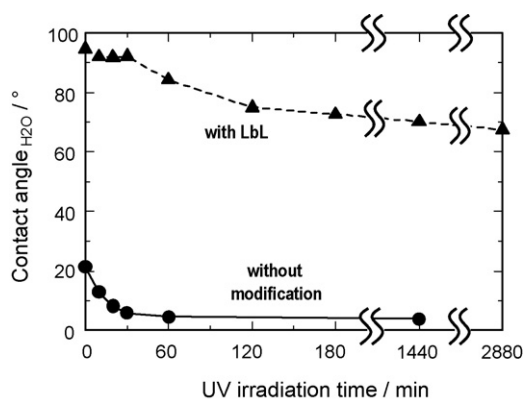


Fig. 8. Changes in contact angle for water of the EPD films prepared from unmodified titanate nanosheets (closed circles) and the LbL-modified titanate nanosheets (closed triangles) with UV irradiation at  $1.0 \text{ mW cm}^{-2}$ .

Structural changes of the LbL-modified titanate nanosheets were investigated via FTIR and XRD measurements. In the FTIR spectra of LbL-modified titanate nanosheets (Fig. 9), absorption bands due to Nafion at about  $1080$  and  $1270 \text{ cm}^{-1}$  can be assigned to C–F bond and  $-\text{SO}_3^-$  group, respectively. PDDA-related absorption bands are present at about  $1520$  and  $1680 \text{ cm}^{-1}$ . These Nafion- and PDDA-related absorption bands were appreciable even after UV irradiation for 120 min. This can be attributed to the lower photocatalytic activity of tetratitanate than of titania crystals such as anatase and rutile, and the higher chemical stability of Nafion and PDDA against pho-

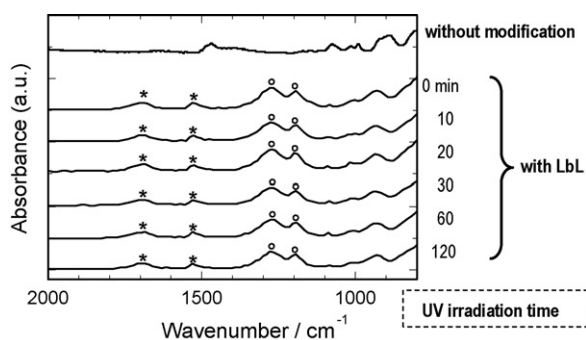


Fig. 9. FTIR spectra of LbL-modified titanate nanosheets irradiated with UV light at  $1.0 \text{ mW cm}^{-2}$ . Open circles and stars are ascribed to Nafion and PDDA, respectively.

tocatalytic oxidation. The surface property evaluated from the contact angle for water is very sensitive to the organic moiety present at the surface of the EPD film, whereas the bulk structure of the LbL-modified titanate nanosheet film should be stable against UV irradiation. In the XRD patterns of the unmodified and LbL-modified titanate nanosheets shown in Fig. 10, reflections due to tetratitanate ( $\text{H}_2\text{Ti}_4\text{O}_9 \cdot x\text{H}_2\text{O}$ ) were observed at about  $8^\circ$ ,  $17^\circ$  and  $26^\circ$ .<sup>14</sup> The diffraction peaks of LbL-modified titanate nanosheets were less intense than those of the unmodified nanosheets, due to the presence of Nafion and PDDA in the LbL-modified titanate nanosheets. For both unmodified and LbL-modified titanate nanosheets, the diffraction peaks became sharper after UV irradiation, which may reflect enhancement of the crystallinity of titanate. A small shift from  $8.48^\circ$  to  $9.70^\circ$  was observed for the main diffraction peak after LbL modification, which corresponds to a decrease in  $d(002)$  from  $1.04$  to  $0.91 \text{ nm}$ . The decrease in  $d$  value after modification is probably due to the decrease in the number of hydration water molecules,  $x$ , in the titanate nanosheets.

Selectivity of the titanate nanosheets for adsorption and photocatalytic decomposition of organics, as well as the compatibility of hydrophobicity and photocatalytic activity, was an important target of the LbL modification in this study. Fig. 11(a) and (b) shows MB and TN adsorption properties in  $10^{-5} \text{ M}$  aqueous solutions for the EPD films prepared from the unmodified and LbL-modified titanate nanosheets, respectively. In the evaluation of adsorption properties for the EPD films, the thickness of the unmodified and LbL-modified films was controlled to about  $2 \mu\text{m}$  by EPD conditions. The ordinate axes of Fig. 11(a) and (b) are absorbance at  $664 \text{ nm}$  for MB and  $599 \text{ nm}$  for TN for the aqueous solutions containing titanate nanosheet EPD films. Both MB solutions showed large decreases in absorbance, *i.e.*, both unmodified and LbL-modified films showed high adsorption capacity for MB (Fig. 11(a)). On the other hand, the LbL-modified EPD film showed higher adsorption capacity for TN than did the unmodified EPD film (Fig. 11(b)). TN is more hydrophobic than MB due to its aromatic character, so that the greater adsorption by the LbL-modified film can be ascribed to hydrophobic interaction between TN and the Nafion/PDDA ion complex formed on titanate nanosheets.

Photocatalytic decomposition and/or bleaching of MB and TN adsorbed on unmodified and LbL-modified EPD films with UV irradiated ( $1 \text{ mW cm}^{-2}$ ) in ambient air are shown

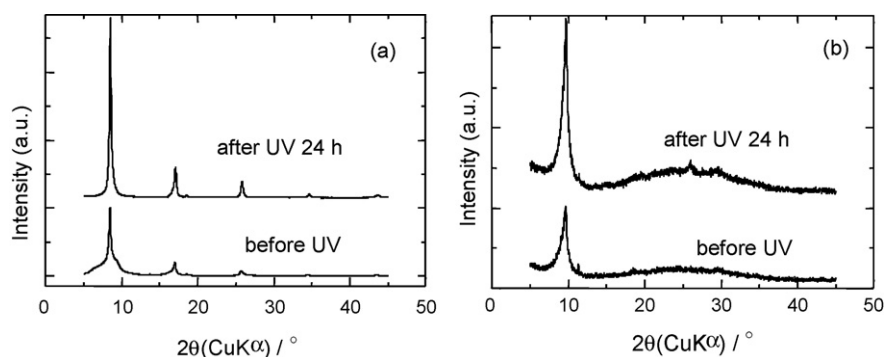


Fig. 10. XRD patterns of the EPD films prepared from (a) unmodified titanate nanosheets and (b) LbL-modified titanate nanosheets before and after UV irradiation at  $1.0 \text{ mW cm}^{-2}$  for 24 h.

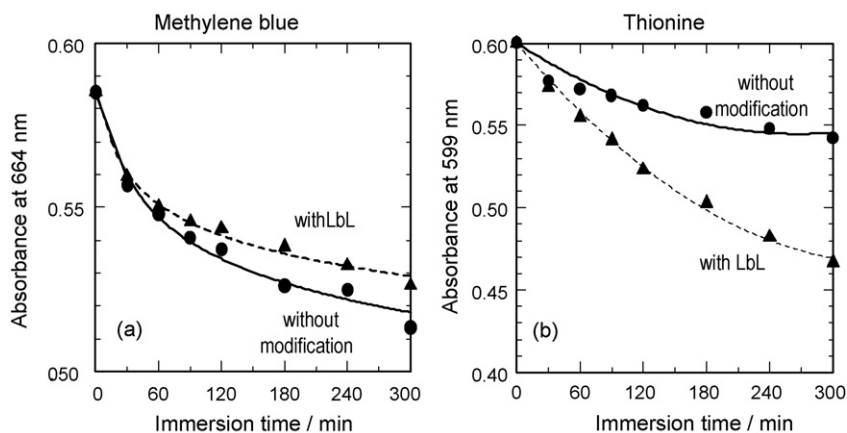


Fig. 11. Adsorption properties of (a) MB and (b) TN in the aqueous solutions of  $10^{-5} \text{ M}$  for the unmodified and LbL-modified EPD films. Closed circles and triangles are for the aqueous solutions containing unmodified and LbL-modified EPD films, respectively.

in Fig. 12(a) (MB) and (b) (TN). The absorption band peak positions ( $\lambda_{\text{max}}$ ) of MB and TN adsorbed on the EPD films shifted from 664 to 605 nm for MB, and from 599 to 547 nm for TN, compared with the MB and TN aqueous solutions. For MB decomposition/bleaching, the absorbance of MB in LbL-modified film is approximately half that in the unmodified film, reflecting the smaller amount of MB adsorbed on the LbL-modified film as shown in Fig. 11(a), and for each

type of film the absorbance decreases substantially with UV irradiation time. On the other hand, in the results for TN decomposition/bleaching, the absorbance of TN in the LbL-modified film is about 4 times that in the unmodified film, which is in accordance with the observation that the amount of TN adsorbed on the LbL-modified film is much larger than that on the unmodified film (see Fig. 11(b)). The absorbance in both cases decreases with UV irradiation time. Most of the TN adsorbed

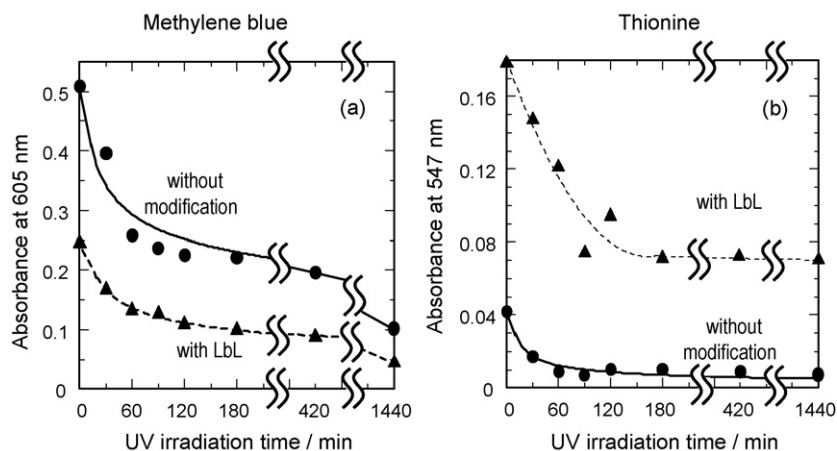


Fig. 12. Photocatalytic decomposition and/or bleaching of (a) MB and (b) TN adsorbed on the unmodified and LbL-modified EPD films with UV irradiation ( $1 \text{ mW cm}^{-2}$ ) in an ambient air. Closed circles and triangles are for unmodified and LbL-modified EPD films, respectively.

on unmodified film was decomposed after UV irradiation for 1440 min, whereas the TN adsorbed on the LbL-modified film was decomposed to a much smaller extent under the same conditions. This suggests that TN molecules near the surface of titanate nanosheet are preferentially decomposed due to the photocatalytic activity of the titanate nanosheet, and there should still exist chemically stable spaces for TN adsorption between the LbL-modified titanate nanosheets. Consequently, selective adsorption and preferential decomposition of hydrophobic substance, and the presence of chemically stable open space for the adsorption in the LbL-modified hydrophobic titanate nanosheets are promising characteristics on which design of functional EPD films can be based.

#### 4. Conclusions

Hydrophobic and photocatalytically active thick films were successfully prepared by EPD on ITO-coated glass substrates from LbL-modified titanate nanosheets. The thickness of the films can be controlled in the range 0.5–8  $\mu\text{m}$  by changing the deposition conditions. Hydrophobicity equivalent to a contact angle for water of  $95^\circ$ , preferential adsorption capability and enhanced photocatalytic activity for hydrophobic substances have been demonstrated. The chemical and structural stabilities of the LbL-modified EPD films have been confirmed by FTIR spectroscopy and XRD. Selective adsorption and preferential decomposition of hydrophobic substances, and the presence of chemically stable open space for adsorption in the LbL-modified hydrophobic titanate nanosheets are promising characteristics on which design of functional EPD films can be based for applications such as environmental purification, self-cleaning, and solar cell electrodes.

#### Acknowledgment

This work was supported by the Ministry of Education, Culture, Sports, Science and Technology (MEXT) of Japan (Grant-in-Aid for Exploratory Research, No. 19656169, 2007–2008 and 20360298, 2008–2009).

#### References

1. Sasaki, T., Ebina, Y., Kitami, Y. and Watanabe, M., Two-dimensional diffraction of molecular nanosheet crystallites of titania oxide. *J. Phys. Chem. B*, 2001, **105**, 6116–6124.
2. Feist, T., Mocarski, S. J., Davies, P. K., Jacobson, A. J. and Lewandowski, J. T., Formation of  $\text{TiO}_2$  (B) by proton exchange and thermolysis of several alkali metal titanate structures. *Solid State Ionics*, 1988, **28–30**, 1338–1343.
3. Sasaki, T., Komatsu, Y. and Fujiki, Y., Protonated pentatitanate: preparation, characterizations, and cation intercalation. *Chem. Mater.*, 1992, **4**, 894–899.
4. Sasaki, T., Watanabe, M., Michiue, Y., Komatsu, Y., Izumi, F. and Take-nouchi, S., Preparation and acid–base properties of protonated titanate with the lepidocite-like layer structure. *Chem. Mater.*, 1995, **7**, 1001–1007.
5. Sasaki, T., Ebina, Y., Tanaka, T., Harada, M., Watanabe, M. and Decher, G., Layer-by-layer assembly of titania nanosheet/polycation composite films. *Chem. Mater.*, 2001, **13**, 4661–4667.
6. Matsuda, A., Matoda, T., Kogure, T., Tadanaga, K., Minami, T. and Tatsumisago, M., Formation and characterization of titania nanosheets-precipitated coatings via sol–gel process with hot water treatment under vibrations. *Chem. Mater.*, 2005, **17**, 749–757.
7. Boccaccini, A. R., Roether, J. A., Thomas, B. J. C., Shaffer, M. S. P., Chavez, E., Stoll, E. et al., The electrophoretic deposition of inorganic nanoscaled materials. *J. Ceram. Soc. Jpn.*, 2006, **114**, 1–14.
8. Kambayashi, T., Daiko, Y., Muto, H., Sakai, M. and Matsuda, A., Electrophoretic deposition and photocatalytic activity of titanate nanosheets. *Key Eng. Mater.*, 2009, **412**, 59–64.
9. Decher, G., Lvov, Y. and Schmitt, J., Proof of multilayer structural organization in self-assembled polyanion molecular films. *Thin Solid Films*, 1994, **244**, 772–777.
10. Ariga, K., Hill, J. P. and Ji, Q., Layer-by-layer assembly as a versatile bottom-up nanofabrication technique for exploratory research and realistic application. *Phys. Chem. Chem. Phys.*, 2007, **9**, 2319–2340.
11. Fujishima, A., Rao, T. N. and Ttyk, D. A., Titanium oxide photocatalysis. *J. Photochem. Photobiol. C: Photochem. Rev.*, 2000, **1**, 1–21.
12. Nakajima, A., Hashimoto, K., Watanabe, T., Takai, K., Yamauchi, G. and Fujishima, A., Photoinduced amphiphilic surface on polycrystalline anatase  $\text{TiO}_2$  thin films. *Langmuir*, 2000, **16**, 7044–7048.
13. Kobayashi, K., Matsuda, A., Kogure, T., Tadanaga, K., Minami, T. and Tatsumisago, M., Hydrophobic and photocatalytically active surface using micropatterns of anatase nanocrystals-dispersed film. *J. Ceram. Soc. Jpn.*, 2004, **112**, S1425–S1429.
14. He, M., Feng, X., Lu, X., Ji, X., Liu, C., Bao, N. and Xie, J., A controllable approach for the synthesis of titanate derivatives of potassium tetratitanate fiber. *J. Mater. Sci.*, 2004, **39**, 3745–3750.